Published in final edited form as:
*Neuron*. 2009 December 10; 64(5): 632–644. doi:10.1016/j.neuron.2009.11.013.

# Overexpression of Low Density Lipoprotein Receptor in the Brain Markedly Inhibits Amyloid Deposition and Increases Extracellular Aβ Clearance

**Jungsu Kim**[1], **Joseph M. Castellano**[1], **Hong Jiang**[1], **Jacob M. Basak**[1], **Maia Parsadanian**[1], **Vi Pham**[1], **Stephanie M. Mason**[1], **Steven M. Paul**[2], and **David M. Holtzman**[1,*]

[1] Department of Neurology, Developmental Biology, Hope Center for Neurological Disorders, Alzheimer's Disease Research Center, Washington University School of Medicine, St. Louis, MO 63110

[2] Eli Lilly & Co., Lilly Research Labs, Indianapolis, IN 46285

## Summary

Apolipoprotein E (*APOE*) is the strongest genetic risk factor for Alzheimer's disease (AD). Previous studies suggest that the effect of apoE on amyloid-β (Aβ) accumulation plays a major role in AD pathogenesis. Therefore, understanding proteins that control apoE metabolism may provide new targets for regulating Aβ levels. LDLR, a member of the LDL receptor family, binds to apoE, yet its potential role in AD pathogenesis remains unclear. We hypothesized that LDLR overexpression in the brain would decrease apoE levels, enhance Aβ clearance and decrease Aβ deposition. To test our hypothesis, we created several transgenic mice that overexpress LDLR in the brain and found that apoE levels in these mice decreased by 50–90%. Furthermore, LDLR overexpression dramatically reduced Aβ aggregation and enhanced Aβ clearance from the brain extracellular space. Plaque-associated neuroinflammatory responses were attenuated in LDLR transgenic mice. These findings suggest that increasing LDLR levels may represent a novel AD treatment strategy.

## INITRODUCTION

Accumulation of the amyloid β peptide (Aβ) in the brain is hypothesized to trigger pathogenic cascades that eventually lead to Alzheimer's disease (AD) (Hardy, 2006). Therefore, strategies modulating production, clearance, and aggregation of Aβ are actively being pursued as disease modifying therapies in AD (Golde, 2006). Aβ peptides are generated by the sequential proteolytic processing of amyloid β precursor protein (APP) by the β- and -secretase (Cole and Vassar, 2007; Sisodia and St George-Hyslop, 2002; Steiner and Haass, 2000). Extensive genetic research on familial AD (FAD) led to the identification of mutations in the *APP*, *presenilin 1 (PSEN1)* and *presenilin 2 (PSEN2)* genes and provided strong support for the critical role of Aβ accumulation in AD pathogenesis (Hardy, 2006). Many research groups have utilized this genetic information to develop transgenic mouse models that recapitulate key pathological phenotypes of AD. These transgenic mice models

*Correspondence: David M. Holtzman, Washington University School of Medicine, Department of Neurology, 660 S. Euclid Ave. Campus Box 8111, St. Louis, MO 63110, holtzman@neuro.wustl.edu, Phone: 1-314-362-9872.

have been useful in understanding the etiology of AD and for testing potential therapeutic approaches for preventing Aβ-dependent pathologies.

Although mutations in FAD-liked genes are known to cause rare forms of FAD, theε4 allele of *apolipoprotein E* (*APOE*) is the only firmly established genetic risk factor for more common forms of AD (Bertram et al., 2007b). ApoE functions as a ligand in the receptor-mediated endocytosis of lipoprotein particles (Kim et al., 2009). After apoE binds to low density lipoprotein (LDL) receptor family members, the ligand-receptor complex is taken up by clathrin-mediated endocytosis and dissociated in endosomes. Upon dissociation, the apoE receptor recycles back to the cell surface, whereas the apoE-containing lipoprotein particle is targeted to the lysosome wherein cholesterol becomes available for cellular needs. Although it is not completely clear how apoE influences the various pathogenic processes implicated in AD, several lines of evidence suggest that the effects of apoE on Aβ aggregation and clearance play a major role in AD pathogenesis (Kim et al., 2009). Previous studies demonstrated that the absence of apoE leads to a dramatic decrease in the levels of fibrillar Aβ deposits in APP transgenic mouse models (Bales et al., 1999; Bales et al., 1997; Holtzman et al., 2000a; Holtzman et al., 2000b). Furthermore, recent studies strongly suggest that apoE regulates both extracellular and intracellular Aβ clearance in the brain (Bell et al., 2007; Deane et al., 2008; DeMattos et al., 2004; Jiang et al., 2008). Therefore, modulating the function of proteins that control apoE metabolism in the brain will likely alter the extent of amyloid deposition and ultimately affect the disease process. In support of this possibility, it was recently demonstrated that ATP-binding cassette transporter A1 (ABCA1)-mediated lipidation of apoE modulates amyloid plaque formation (Hirsch-Reinshagen et al., 2005; Koldamova et al., 2005; Wahrle et al., 2005; Wahrle et al., 2008). Consequently, further insight into how apoE levels can be regulated in the brain may lead to novel therapeutic avenues for the prevention and treatment of AD.

ApoE binds to a group of structurally related proteins known as the low density lipoprotein receptor (LDLR) family. This family includes LDLR, lipoprotein receptor-related protein 1 (LRP1), lipoprotein receptor with 11 binding repeats (LR11), apolipoprotein receptor 2 (ApoER2), very low density lipoprotein receptor (VLDLR) and others (Herz and Bock, 2002). They share several common structural characteristics, such as complement-type ligand binding repeats, β-propeller domain, and epidermal growth factor type repeats. The prototype of this family member is LDLR, which has been extensively studied in the peripheral tissues for its role in mediating the removal of cholesterol and cholesteryl ester from the circulation (Brown and Goldstein, 1986). Genetic defects in LDLR lead to an impaired lipoprotein clearance from the bloodstream and massive accumulation of cholesterol in the circulation, resulting in familial hypercholesterolemia. Due to its critical role in the metabolism of apoB-containing LDL particles, LDLR has been the focus of much attention in better understating the pathogenesis of atherosclerosis and coronary heart disease (Soutar and Naoumova, 2007). However, the physiological and pathological function of LDLR in the nervous system remains unclear. In contrast, the roles of other LDL receptor family members in brain development and synaptic plasticity are better understood (Herz, 2009). Furthermore, the modulatory effects of other LDL receptors on Aβ clearance and APP trafficking have been thoroughly examined in cellular and animal model systems (Cam and Bu, 2006). However, the potential role of LDLR in AD pathogenesis has not been studied extensively. To address this issue, we created several transgenic mouse lines that overexpress LDLR in the brain and bred two transgenic lines with the APPswe/PSEN1ΔE9 (APP/PS1) transgenic mouse model (Jankowsky et al., 2004). The effects of LDLR overexpression on Aβ accumulation and its clearance from the brain interstitial fluid (ISF) were investigated.

# RESULTS

## Generation and Characterization of LDLR Transgenic Mice

In order to achieve widespread expression of the LDLR transgene in the brain, we created a construct using the mouse prion promoter (Borchelt et al., 1996). Six transgenic founders with LDLR transgene were generated and maintained on a B6/CBA background. One transgenic line transmitted the LDLR transgene only in males and did not have any detectable transgene expression in the brain. The five remaining transgenic lines were screened for LDLR overexpression by western blotting (Figure 1A). As expected, multiple bands of LDLR proteins were detected due to extensive posttranslational modifications (Filipovic, 1989). Two to eleven fold increases in LDLR protein levels, relative to non-transgenic (NTG) mice, were detected in the various founder lines (Figure 1A). The high-expressing B line and low-expressing E line were selected for further experiments.

To characterize the regional expression pattern of the LDLR transgene, brain sections were immunostained using an anti-hemagglutinin (HA) antibody for the detection of the HA tag placed in the amino-terminal region of the LDLR sequence. As expected, the immunostaining pattern with anti-HA antibody overlapped very well with that of anti-LDLR antibody staining (Figure S1). Transgene expression, analyzed by anti-HA antibody, was detected in cortex, hippocampus, and cerebellum (Figure 1B–1D). Double immunofluorescence staining with anti-NeuN, a neuron-specific marker, and anti-HA antibody demonstrated that most neurons expressed LDLR from the transgene (Figure 1E). To further examine which cell types express the transgene, primary neurons or astrocytes were cultured from LDLR transgenic line B mice. LDLR expression was analyzed with anti-LDLR antibody or anti-HA antibody (Figure 1F–1G). Higher levels of LDLR protein were detected in both neurons and astrocytes. This expression pattern is consistent with a previous study characterizing the prion promoter expression vector (Borchelt et al., 1996).

To analyze the functional effect of LDLR overexpression in the brain, the levels of apoE protein in the brain was analyzed by apoE enzyme-linked immunosorbent assay (ELISA). Since LDLR is one of the major apoE endocytic receptors in the brain (Fryer et al., 2005), we expected that LDLR overexpression would lead to a reduction in apoE protein levels through enhanced receptor-mediated endocytosis. There was a significant decrease in apoE protein levels in all five lines, ranging from 50 to 90%, compared to NTG littermates (Figure 2A). Interestingly, only two-fold overexpression in LDLR transgenic line E mice was sufficient to decrease apoE levels by ~50% in the brain. Overexpression of LDLR by more than five-fold, relative to NTG mice, led to 80–90% reduction in apoE levels. We also analyzed apoE mRNA levels by quantitative RT-PCR. There were no significant differences in apoE mRNA levels between LDLR transgenic lines B (> 10-fold overexpression) and E (2-fold overexpression) and their NTG littermates (Figure S2). This suggests that the higher levels of LDLR in the transgenic mice facilitate apoE endocytosis from the extracellular space, leading to a decrease in the amount of extracellular apoE.

The higher levels of LDLR in the transgenic mice may facilitate apoE endocytosis from the extracellular space, leading to a decrease in the amount of extracellular apoE.

## LDLR Overexpression Decreases ApoE Levels Even in the Presence of APPswe and PSEN1ΔE9 Overexpression

A recent study demonstrated that the APP intracellular domain may increase apoE protein levels by suppressing the transcription of LRP1, another major apoE receptor in the brain (Liu et al., 2007). Furthermore, altered γ-secretase activity by a PSEN1ΔE9 mutation has been shown to increase apoE protein levels by interfering with the endocytosis of LDLR (Tamboli et al., 2008). Therefore, we evaluated the possibility that overexpression of APP

and PSEN1ΔE9 in APP/PS1 transgenic mice used in our study might attenuate the effect of LDLR overexpression on apoE levels. To determine whether LDLR overexpression still has a functional effect on apoE protein in the presence of the APP and PSEN1E9 transgenes, soluble apoE levels were analyzed from APP/PS1/LDLR and APP/PS1 transgenic mice at 2.5 months of age. ApoE levels in cortical and hippocampal tissues from LDLR line B transgenic mice were significantly decreased by ~90%, compared with NTG mice (Figure 2B). In the low-expressing line E transgenic mice, there was a 55–60% reduction of apoE protein levels in both cortex and hippocampus (Figure 2C). The effect size of LDLR overexpression on apoE protein levels was not different in the absence (Figure 2A) or presence (Figure 2B and 2C) of APP and PSEN1ΔE9 overexpression. Taken together, these results strongly suggest that overexpression of APP and PSEN1ΔE9 does not interfere with the function of LDLR in our transgenic mice. In addition to the strong effect of the LDLR transgene on apoE levels, there was also a sex difference in apoE protein levels. In the absence of LDLR transgene overexpression, male APP/PS1 mice had 10–20% less apoE protein in the cortex and hippocampus compared with female littermates ($p=0.05$ and $p=0.06$ for B line Ctx and Hip, respectively, $p=0.02$ and $p=0.0008$ for E line Ctx and Hip, respectively) (Figure 2B and 2C). The difference in apoE protein levels between female and male mice was unlikely due to differences in endogenous LDLR protein levels, since LDLR levels were not significantly different between female and male APP/PS1 mice (Figure S3C).

Previous studies suggest that there may be functional redundancy among LDL receptor family members (Mahley and Ji, 1999; Wouters et al., 2005). Apolipoprotein J (ApoJ) and ApoE are the two most abundant apolipoproteins in the brain. ApoJ, also known as clusterin, has been shown to facilitate fibrillar amyloid plaque formation (DeMattos et al., 2002). To determine whether LDLR overexpression had a selective effect on apoE, we assessed apoJ protein levels by western blot analysis. No significant difference in the levels of apoJ was found between LDLR transgenic and NTG mice (Figure S3B). This finding suggests that even more than 10-fold overexpression of LDLR does not affect the metabolism of a similar apolipoprotein.

## Strong LDLR Overexpression Leads to Marked Decreases in Amyloid Deposition

Previous studies demonstrated that the lack of apoE led to a dramatic decrease of amyloid deposition in APP transgenic mouse models (Bales et al., 1997; Holtzman et al., 2000b). Given the critical role of apoE in Aβ deposition, we hypothesized that the reduction of extracellular apoE levels by LDLR overexpression may lead to a decrease in Aβ accumulation. To determine whether LDLR overexpression affects Aβ accumulation and deposition, the high-expressing LDLR transgenic line B mice were bred with APP/PS1 transgenic mice. The extent of Aβ deposition was analyzed by histochemical and biochemical methods. Brain sections from 7 month old APP/PS1 mice (Figure 3A and 3C) and APP/PS1/LDLR mice (Figure 3B and 3D) were immunostained with biotinylated-3D6 antibody (anti-Aβ 1–5).

In our preliminary studies with APP/PS1 transgenic mice, there was a significant difference in amyloid plaque load between female and male mice. Therefore, we planned to analyze the extent of Aβ accumulation by sex in this study. In the absence of LDLR overexpression, male APP/PS1 mice had a 50–60% decrease in amyloid plaque load, compared with female APP/PS1 littermates ($p=0.0087$ and $p=0.0022$ for Ctx and Hip, respectively) (Figure 3E). Quantitative analyses of anti-Aβ immunostaining demonstrated that amyloid plaque loads in the cortex and hippocampus were markedly decreased in APP/PS1/LDLR transgenic mice compared with APP/PS1 mice (Figure 3E). The inhibitory effects of LDLR overexpression on Aβ accumulation were observed in both female and male mice.

To further characterize the nature of the deposited plaques, brain sections were subsequently stained with X-34 dye that detects fibrillar amyloid deposits. In line with the results from Aβ immunostaining (Figure 3E), there were strong sex differences in fibrillar amyloid deposition. Female APP/PS1 mice deposited significantly more fibrillar plaques than did male APP/PS1 littermates ($p=0.0234$ and $p=0.0087$ for Ctx and Hip, respectively) (Figure 3F). Importantly, APP/PS1/LDLR transgenic mice exhibited a dramatic 40–70% decrease in the X-34 positive fibrillar plaque load in the cortex and hippocampus, compared with sex-matched APP/PS1 mice (Figure 3F). Consistent with the histochemical analyses, biochemical analyses of Aβ levels demonstrated a 50–75% reduction in insoluble Aβ40 levels (Figure 4A) and a 45–70% reduction in insoluble Aβ42 levels in the cortex and hippocampus of APP/PS1/LDLR transgenic mice (Figure 4B). Taken together, our results from high-expressing LDLR transgenic line B mice demonstrate that 10-fold LDLR overexpression markedly decreases Aβ accumulation and amyloid deposition.

## Two-fold Overexpression of LDLR is Sufficient to Inhibit Amyloid Formation

To determine whether lower levels of LDLR overexpression would also have a protective effect against Aβ accumulation and deposition, LDLR transgenic line E mice that overexpress LDLR by approximately 2-fold were bred to APP/PS1 transgenic mice. Levels of Aβ accumulation were analyzed by anti-Aβ immunohistochemistry and X-34 staining (Figures 5A and 5B). Amyloid plaque loads in the cortex and hippocampus were markedly lower in female APP/PS1/LDLR transgenic mice, compared with female APP/PS1 mice (Figure 5C). In addition, female APP/PS1/LDLR mice had a 50–55% decrease in fibrillar plaque load in the cortex and hippocampus (Figure 5D). In line with the histochemical findings, biochemical measurement of Aβ levels demonstrated a 30–55% reduction in total (soluble plus insoluble) Aβ40 levels and an approximately 35% reduction in total Aβ42 levels in the cortex and hippocampus of APP/PS1/LDLR transgenic mice (Table S1). In contrast to the effects in females, there was no significant difference between plaque load or Aβ levels in male APP/PS1 versus APP/PS1/LDLR transgenic mice from line E. Collectively, these findings strongly suggest that even a small increase of LDLR protein levels can be effective in preventing Aβ accumulation in female mice (Figure 5C and 5D).

## Attenuation of Neuroinflammatory Responses in APP/PS1/LDLR Transgenic Mice

Abnormal activation of microglia and astrocytes is observed in the brains of AD patients and transgenic mouse models of amyloidosis (Wyss-Coray, 2006). Previous studies suggest that fibrillar amyloid plaques may trigger neuroinflammatory cascades (Meyer-Luehmann et al., 2008). To quantitatively examine the extent of gliosis, we established a semi-automated imaging processing method and assessed the activation of microglia by using CD11b (Figure 6A and 6B) and CD45 (Figure 6D and 6E) as markers. There was an ~70% decrease in the CD11b-positive activated microglial load in APP/PS1/LDLR line B transgenic mice, compared with APP/PS1 littermates (Figure 6C). Similarly, analysis of CD45-positive microglia indicated an ~80% reduction in area covered by activated microglia in LDLR transgenic mice (Figure 6F). In addition, brain sections were stained with anti-glial fibrillary acidic protein (GFAP) antibody to quantify the extent of astrogliosis (Figure 6G and 6H). Clusters of activated astrocytes were often associated with amyloid plaques (Figure S4A). APP/PS1/LDLR transgenic mice had ~45% less GFAP load in cortex, compared with APP/PS1 littermates (Figure 6I). The extent of microgliosis and astrogliosis were correlated very well with the amount of compact fibrillar plaques detected with the X-34 dye (Figure S4B–S4D). These findings demonstrate that the reduction of fibrillar plaque formation by LDLR overexpression is closely associated with the decreased activation of microglia and astrocytes.

### LDLR Overexpression Decreases Steady-state ISF eAβ Levels in Young Mice and Increases the Elimination of eAβ from the ISF

We reasoned that the marked reduction in Aβ deposition in mice overexpressing LDLR may be the result of altered soluble Aβ metabolism early in life in the extracellular space of the brain where it is prone to aggregate (Meyer-Luehmann et al., 2003). To assess this possibility, we performed in vivo microdialysis in APP/PS1/LDLR line B transgenic mice and APP/PS1 littermates prior to the onset of amyloid deposition to compare levels of soluble Aβ in the hippocampal ISF. Soluble ISF Aβ exchangeable across a 38kDa dialysis membrane (eAβ) has previously been shown to be tightly correlated with the levels of total soluble Aβ present in extracellular pools of the brain (Cirrito et al., 2003). Theoretically, the actual in vivo steady state concentration of an analyte being dialyzed exists at the point at which there is no flow of the perfusion buffer (Menacherry et al., 1992). To obtain this value, we varied the flow rate of the perfusion buffer from 0.3μL/min to 1.6μL/min during microdialysis in the hippocampus of young APP/PS1/LDLR and APP/PS1 mice (Figure 7A1). After extrapolating back to the point of zero flow for each mouse, we found that the mean steady state concentration of ISF $eA\beta_{1-x}$ was significantly lower in APP/PS1/LDLR mice compared to mice expressing normal levels of LDLR (Figure 7A2). This difference was not due to differential recovery of eAβ by the probe between groups at any of the flow rates tested (Figure S5). Since the extent of Aβ deposition observed in Figure 3 was found to depend on the sex of the mice analyzed, we stratified microdialysis experiments in the same way. We found that both male and female APP/PS1 mice overexpressing LDLR had lower steady state ISF $eA\beta_{1-x}$ levels compared to their sex-matched APP/PS1 counterparts (Figure 7A3). Though we did not observe a similar change in Aβ levels as assessed by conventional biochemical means (Table S2), it is likely that the Aβ sampled during in vivo microdialysis more closely reflects the extracellular pool than total Aβ measured from tissue homogenates.

Given that LDLR overexpression did not appear to alter APP processing (Figure S3B), and based on our previous finding that apoE decreased the elimination rate of soluble Aβ from the ISF (DeMattos et al., 2004), we hypothesized that the lower steady state concentration of eAβ in APP/PS1/LDLR mice is likely the result of increased elimination from the brain ISF (Deane et al., 2008; DeMattos et al., 2004). To test this hypothesis, we injected young APP/PS1 and APP/PS1/LDLR mice intraperitoneally with a potent γ-secretase inhibitor in order to halt Aβ production, thus allowing sensitive measurement of the elimination rate of eAβ from the ISF, as previously described (Figures 7B1 and 7B2) (Cirrito et al., 2003; DeMattos et al., 2004). The half-life of elimination from the ISF for $eA\beta_{1-x}$ was decreased by about two-fold in APP/PS1/LDLR mice compared to that measured in APP/PS1 mice (Figure 7B3). The increase of eAβ elimination in LDLR transgenic mice was observed in both males and females (Figure 7B4). Taken together, these results demonstrate that increasing expression of LDLR promotes the elimination of soluble Aβ from the ISF, leading to lower levels of the peptide in the hippocampal extracellular space. It is likely that the enhanced Aβ elimination from the ISF early in the life of the mice underlies the resulting strong decrease in Aβ accumulation and its consequences such as inflammation that progress with age.

## DISCUSSION

In the current study, we hypothesized that overexpression of LDLR in the brain would decrease brain apoE protein levels, subsequently decreasing amyloid deposition. To test this hypothesis, we created several transgenic mouse lines that overexpress LDLR in the brain and then bred them with APP/PS1 transgenic mice. Brain apoE levels in LDLR transgenic mice were decreased by 50–90% in a dose-dependent manner. Most importantly, LDLR overexpression led to dramatic reductions in Aβ aggregation and neuroinflammatory responses. In addition, increasing expression of LDLR facilitated the elimination of soluble Aβ from the ISF, leading to lower levels of Aβ in the hippocampal extracellular space. This

result strongly suggests that LDLR enhances brain Aβ clearance, serving as an important pathway that modulates Aβ metabolism. Overall, the results suggest that LDLR may be an attractive therapeutic target for AD.

Although numerous putative susceptibility genes for AD have been reported so far, the strongest genetic risk factor is *APOE* genotype; the ε4 allele is an AD risk factor and the ε2 allele appears to be protective (Bertram et al., 2007b). Given the considerable genetic evidence and the immunoreactivity of apoE in amyloid plaques, the effect of apoE isoforms on Aβ aggregation has been investigated extensively in vitro (Kim et al., 2009). Later, in vivo studies demonstrated that the lack of apoE led to a dramatic reduction of fibrillar Aβ deposition in APP transgenic mouse models (Bales et al., 1999; Bales et al., 1997; Holtzman et al., 2000a; Holtzman et al., 2000b). Furthermore, apoE has been shown to regulate Aβ clearance in the brain (Bell et al., 2007; Deane et al., 2008; DeMattos et al., 2004; Jiang et al., 2008). These and other findings strongly suggest that the effects of apoE on Aβ aggregation and clearance play a major role in AD pathogenesis (Kim et al., 2009). Consequently, modulating the function or levels of proteins that affect apoE metabolism in the brain seems to be a logical therapeutic strategy to alter Aβ-dependent pathogenic processes in AD. Results presented in the current study corroborate the feasibility and efficacy of apoE targeting therapeutics.

ApoE in the periphery is known to bind to several LDL receptor family members. Since the lipid composition and lipidation state of apoE-containing lipoprotein particles are different between brain and peripheral tissues, it would be important to know which LDL receptor members can regulate apoE protein levels in the brain (Kim et al., 2009). Knockout mouse studies have provided direct evidence for LDLR and LRP1 as major apoE receptors in the brain (Elder et al., 2007; Fryer et al., 2005; Liu et al., 2007). Fryer et al. also demonstrated that LDLR differentially regulates the levels of human apoE isoforms in the brain through its binding specificity. Zerbinatti et al. generated a LRP1 mini-receptor transgenic mouse model with 3.7-fold increased LRP1 levels in the brain (Zerbinatti et al., 2004). Although an ~25% reduction in brain apoE levels was observed in LRP1 transgenic mice, there was an increase in soluble and insoluble Aβ in old mice (Zerbinatti et al., 2006; Zerbinatti et al., 2004). The reason for the LRP1 mini-receptor overexpression causing an increase in Aβ levels is not entirely clear but is likely due to the effects of LRP1 on APP and not due to its effects on apoE. For example, unlike LDLR, LRP1 is an APP binding protein that influences APP endocytic trafficking and cellular distribution such that processing to Aβ and its extracellular release is enhanced (Pietrzik et al., 2002; Ulery et al., 2000). This effect of LRP1 on APP and Aβ may supersede the effects of the LRP1 minireceptor on decreasing apoE levels by 25% and its effects on Aβ in the brain. In the current study, only 2-fold overexpression of LDLR protein was sufficient to decrease brain apoE levels and Aβ accumulation by more than 50%. Taken together, these data clearly demonstrate both LDLR and LRP1 regulate apoE protein levels in the brain. However, it is unclear whether other LDL receptor family members, such as LR11, ApoER2, and VLDLR, also efficiently mediate the endocytosis of apoE in the brain. Given the known apoE isoform-specific interactions with LDLR (Kim et al., 2009), it would be interesting to determine whether the effect of LDLR overexpression differs in APP transgenic mouse models with humanized apoE isoforms. In addition, it will be important to determine the effects of LDLR overexpression on cognitive abnormalities observed in APP/PS1 mice.

Although the effects of LRP1 on Aβ clearance and APP processing have been extensively studied (Cam and Bu, 2006), the potential role of LDLR on AD pathogenesis has been unclear. Several studies reported that a few single-nucleotide polymorphisms (SNPs) in *LDLR* gene are associated with the risk of developing AD in case-control studies (Cheng et al., 2005; Gopalraj et al., 2005; Retz et al., 2001). However, others could not replicate the

earlier studies and a meta-analysis of the previously reported case-control data failed to detect any significant summary odds ratios (Bertram et al., 2007a; Rodriguez et al., 2006). More recent findings suggest that other SNPs may be associated with a risk of AD in a sex-specific manner. SNP rs688 and haplotype GTT were significantly associated with an increased risk of AD in males and females, respectively (Lämsä et al., 2008; Zou et al., 2008). Unlike other studies, both studies also demonstrated functional effects of SNPs on LDLR splicing and Aβ42 levels.

In order to investigate the effect of LDLR deficiency on cholesterol and Aβ in the brain, several groups have analyzed LDLR knockout mice. Although LDLR deficiency significantly increased murine brain apoE levels by ~50%, it did not alter brain cholesterol levels (Elder et al., 2007; Fryer et al., 2005; Quan et al., 2003; Taha et al., 2008). Previously, we demonstrated that there was no significant change in brain Aβ levels both before and after the onset of amyloid deposition in PDAPP transgenic mice on a LDLR-deficient background (Fryer et al., 2005). However, there was a trend for an increase in Aβ accumulation in PDAPP/LDLR knockout mice. Recently, Buxbaum and colleagues also reported that LDLR deficiency did not affect endogenous murine Aβ levels in the brain (Elder et al., 2007). In contrast, lack of LDLR was associated with increased amyloid deposition in Tg2576 mice (Cao et al., 2006).

Prior to our current study, it was unknown whether increased levels of LDLR in the brain would affect Aβ accumulation in vivo, and if so, via what mechanism. Given the role of apoE in Aβ clearance and aggregation, we hypothesized that the reduction of apoE levels by LDLR overexpression would promote the elimination of soluble Aβ from the brain ISF, i.e., via transcytosis across the blood-brain barrier into the plasma or by local cellular uptake and degradation within the brain. We predicted that increased elimination of soluble Aβ through either of these elimination routes would result in decreased Aβ accumulation. Our in vivo microdialysis results suggest that the mechanism by which LDLR overexpression alters Aβ metabolism is to enhance the extracellular clearance of Aβ peptide. It is possible that receptor-mediated clearance of Aβ-ApoE complex or Aβ alone from the brain ISF might be enhanced by LDLR overexpression. Interestingly, other LDL receptor family members, such as LRP1, LR11, and ApoER2, are known to directly or indirectly bind to APP and affect its amyloidogenic processing (Kim et al., 2009). Since levels of carboxyl-terminal fragments of APP, generated by APP processing, were not different between genotypes, it is unlikely that LDLR overexpression alters APP processing. Though it is likely that the reduction of apoE protein levels by LDLR overexpression enhanced Aβ clearance (DeMattos et al., 2004), we cannot exclude the possibility that LDLR may directly affect Aβ clearance independent of apoE.

Transgenic mouse models of amyloidosis have been invaluable for investigating AD pathogenic mechanisms and evaluating the efficacy of novel therapeutic targets. Interestingly, female APP/PS1 transgenic mice used in the current study had a more than 2-fold increase in plaque load and insoluble Aβ accumulation, compared with male littermates (Figure 3 and 4). Our finding is consistent with a recent study that used APP/PS1 mice on a different genetic background (Halford and Russell, 2009). A similar sex-specific amyloid deposition phenotype has been previously reported with other APP transgenic mouse models (Callahan et al., 2001;Wang et al., 2003). The APP/PS1 transgenic mouse used in our study is one of the most commonly used Aβ amyloidosis models. Effects of genetic and pharmacological manipulations on Aβ accumulation and Aβ-related pathological changes have been tested using this model. However, most previous studies did not analyze the extent of Aβ accumulation by sex. It is possible that sex differences were not obviously recognized in other studies due to the limited sample size for each sex. Given the dramatic effect of sex on Aβ aggregation, the sex of APP/PS1 transgenic mice should be carefully

considered for the proper interpretation of results. Since the prevalence of AD is higher in women even after adjusting for age and education levels (Andersen et al., 1999), it is intriguing that several mouse models of amyloidosis have similar sex-dependent phenotypes. Several studies suggest that female hormones may, in part, contribute to sex differences in AD (Carroll et al., 2007;Yue et al., 2005). Given the inconsistent findings among studies, the exact mechanism underlying sex differences in AD pathogenesis requires further investigation. It is possible that the elevated apoE levels in the females APP/PS1 mice is related to why females develop more amyloid deposition (Figure 2). Interestingly, while the clearance of soluble Aβ in APP/PS1 males trended towards being faster than that for APP/PS1 females (Figure 7B4), we cannot rule out that an Aβ clearance-independent mechanism may account for the sex differences in plaque load and insoluble Aβ accumulation in older mice. Understanding the factors that regulate sex-dependent phenotypes may provide additional insight into new therapeutic targets.

Notably, an increase of LDLR protein levels by only ~2-fold was sufficient to decrease Aβ accumulation by ~50% in APP/PS1 female transgenic mice. Our findings suggest that even a small increase in LDLR levels or function in the brain may be exploited as a novel approach for developing AD therapeutics. Due to the critical role of LDLR in the metabolism of apoB-containing LDL particles in the circulation, strategies increasing the function and amount of LDLR protein in the liver have been extensively pursued as promising therapies for atherosclerosis and premature coronary heart disease (Soutar and Naoumova, 2007). Overexpression of LDLR in the liver facilitated LDL elimination by receptor-mediated endocytosis and prevented diet-induced hypercholesterolemia (Hofmann et al., 1988; Yokode et al., 1990). However, the modulation of LDLR function in the brain as a treatment modality for AD has not been previously investigated. Our study clearly demonstrates the beneficial effects of LDLR overexpression in the brain on pathogenic Aβ aggregation and subsequent neuroinflammatory responses. Although other LDL receptor family members bind to multiple ligands (i.e. LRP1 having more than 20 ligands), there are only two known ligands, apoB and apoE, for LDLR. Since apoB is not expressed in the brain, modulating LDLR function in the brain is likely to target apoE specifically. A couple of recently identified genes are known to regulate LDLR protein levels by affecting the trafficking and degradation of LDLR in peripheral tissues (Soutar and Naoumova, 2007). Since these proteins are also expressed in the brain, their potential roles in the clearance and accumulation of Aβ warrant further investigations. In addition, several compounds have been identified to increase hepatic LDLR protein levels by modulating synthesis or degradation of LDLR and LDLR-regulating proteins. Given our results from transgenic mice overexpressing LDLR in the brain, the therapeutic potential of these lead compounds merit additional testing in animal models of Aβ amyloidosis.

## EXPERIMENTAL PROCEDURES

### Generation of LDLR Transgenic Mice

Murine *LDLR* was cloned from RNA isolated from mouse brain using the RNeasy kit (QIAGEN). Random primer RT-PCR was performed using the First Strand cDNA Synthesis Kit (Roche Applied Sciences). The sequence and orientation of the insert was verified by complete sequencing. *LDLR* cDNA was excised from pcDNA3.1 using XhoI and inserted into the cloning site of the mouse prion promoter vector (Borchelt et al., 1996), a gift from David Borchelt (University of Florida). The Mouse Genetics Core Laboratory at Washington University produced the transgenic mice on a B6/CBA background. Among 6 transgenic founders, 2 lines of LDLR transgenic mice were crossed with APPswe/PSEN1ΔE9 (APP/PS1) transgenic mice (line 85, Stock number 004462, The Jackson Laboratory). APP/PS1 transgenic mice overexpress a chimeric mouse/human *APP695* swedish gene and human *PSEN1* with an exon 9 deletion (Jankowsky et al., 2004). All

comparisons between APP/PS1 transgenic mice with or without an LDLR transgene were littermates on the same genetic background.

### Primary Astrocyte Cultures

Cortical primary murine astrocytes were obtained from P2 mouse pups. Cortices were dissected from the brain and placed in Hanks balanced salt solution then treated with trypsin/EDTA. Following trypsin digestion, the tissue was resuspended and triturated in growth media containing DMEM/F12, 20% fetal bovine serum (FBS), 10 ng/ml epidermal growth factor, 100 units/ml penicillin/streptomycin, and 1 mM sodium pyruvate. The cell suspension was then passed through a 100 μm nylon filter and plated into T75 flasks coated with poly-D-lysine. Once the cells reached confluency, they were shaken at 100 rpm for three hours and the media was aspirated to remove the less adherent microglial cells. The cells were then passaged into 6 well plates for experiments.

### Primary Neuron Cultures

Cortical primary murine neurons were obtained from E16 embryos. Cortices were dissected from the brain, cut into small pieces, and placed into HBSS. The tissue was then treated with trypsin/EDTA for 15 min at 37°C. FBS was then added to the tissue, and it was washed with HBSS (without calcium and magnesium). Following the wash steps, the tissue was resuspended in HBSS (-calcium/magnesium) and 500 U/mL of DNase I. The tissue was then triturated and the cells were resuspended in neurobasal medium with 10% FBS. Cells were then counted and plated into 6 well plates. 3 hrs following the plating, the seeding medium was replaced with neurobasal medium containing B27 supplement. To remove contaminating glial cells, a mixture of antimitotics (5-fluoro-2′-deoxyuridine, uridine, and cytosine β-D-arabinofuranoside) was added to the cultures on DIV5. The media was then changed to neurobasal media with B27 on DIV7.

### Quantitative Analyses of Amyloid Deposition

Brain hemispheres were placed in 30% sucrose before freezing and cutting on a freezing sliding microtome. Serial coronal sections of the brain at 50 mm intervals were collected from the rostral anterior commisure to caudal hippocampus as landmarks. Sections were stained with biotinylated 3D6 (anti-Aβ1–5) antibody or X-34 dye. Stained brain sections were scanned with a NanoZoomer slide scanner (Hamamatsu Photonics). For quantitative analyses of 3D6-biotin staining, scanned images were exported with NDP viewer software (Hamamatsu Photonics) and converted to 8-bit grayscale using ACDSee Pro 2 software (ACD Systems). Converted images were thresholded to highlight plaques and then analyzed by “Analyze Particles” function in the ImageJ software (National Institutes of Health) (Kim et al., 2007). Identified objects after thresholding were individually inspected to confirm the object as a plaque or not. X-34 stained sections were quantified following unbiased stereological principles (Cavalieri-point counting method) (Holtzman et al., 2000b). Three brain sections per mouse, each separated by 300 μm, were used for quantification. These sections correspond roughly to sections at Bregma −1.7, −2.0, and −2.3 mm in the mouse brain atlas. The average of 3 sections was used to represent a plaque load for each mouse. For analysis of Aβ plaque in the cortex, the cortex immediately dorsal to the hippocampus was assessed. All analyses were performed in a blinded manner.

### Sandwich ELISA for Aβ and ApoE

Cortical and hippocampal tissues were sequentially homogenized with PBS and 5M guanidine buffer in the presence of 1x protease inhibitor mixture (Roche). The levels of Aβ and ApoE were measured by sandwich ELISA. For Aβ ELISA, HJ2 (anti-Aβ35–40) and HJ7.4 (anti-Aβ37–42) were used as capture antibodies and HJ5.1-biotin (anti-Aβ13–28) as

the detection antibody. WUE4 (Krul et al., 1988) and anti-ApoE antibody (Calbiochem) were used for apoE ELISA. Pooled C57BL/6J plasma was used as a standard for murine apoE quantification (Fryer et al., 2005). For in vivo microdialysis experiments, human $A\beta_{1-x}$ from collected fractions was measured using m266 antibody (anti-Aβ13–28) to capture and 3D6-biotinylated antibody (anti-Aβ1–5) to detect.

### Quantitative Analyses of Neuroinflammatory Response

Brain sections cut with a freezing sliding microtome were immunostained with anti-CD11b antibody (BD Pharmingen), anti-CD45 antibody (Serotec), and anti-GFAP antibody (Chemicon). The percent area covered by CD11b and CD45 staining was analyzed in the hippocampus by using NDP viewer, ACDSee Pro 2, and NIH Image J softwares, as described above. For GFAP quantification, cortical regions were assessed. The overall area covered by GFAP staining signals was measured with NDP viewer. Three brain sections per mouse, each separated by 300 μm, were used for quantification. The average of 3 sections was used to estimate the area covered by immunoreactivity with each antibody. All analyses were performed in a blinded manner.

### Western Blot

Cortical tissues, primary neurons, and astrocytes cultures were sonicated in radioimmunoprecipitation assay (RIPA) buffer (1% NP-40, 1% sodium deoxycholate, 0.1% SDS, 25mM Tris-HCl, 150mM NaCl) or 1% Triton X-100 in the presence of 1x protease inhibitor mixture (Roche). Cortical tissue homogenates were centrifuged at 18,0000 rcf for 30 min. Primary cells were spun down at 14,000 rcf for 15 min. Protein concentration in supernatants was determined using the BCA protein assay kit (Pierce). Equal amounts of protein for each sample were run on 3–8% Tris-Acetate or 4–12% Bis-Tris XT gels (Bio-Rad) and transferred to PVDF membranes. Blots were probed for LDLR (Novus, Abcam, and a gift from Dr. Guojun Bu at Washington University), CT22 (Zymed), HA (Covance) and ApoJ (Covance). Normalized band intensity was quantified using NIH ImageJ software (Kim et al., 2007).

### In Vivo Microdialysis

In vivo microdialysis in 2.5 month old APP/PS1 and APP/PS1/LDLR (B-line) littermates was performed essentially as described (Cirrito et al., 2003; DeMattos et al., 2004). Briefly, microdialysis using the zero flow extrapolated method was performed with an automated syringe pump (Univentor 864) connected to a laptop using Univentor 300 software. Zero flow data for each mouse were fit with an exponential decay regression as described (Menacherry et al., 1992). For clearance experiments, a stable baseline of ISF eAβ levels was obtained using a constant flow rate of 1.0μl/min before intraperitoneally injecting each mouse with 10 mg/kg of the gamma secretase inhibitor LY411,575 (prepared by dissolving in PBS and propylene glycol). The elimination of eAβ from the ISF followed first -order kinetics; therefore, for each mouse, the elimination half-life for eAβ was calculated using the slope of the linear regression that included all fractions until levels stopped decreasing.

### Statistical Analyses

To determine the statistical significance (*$p<0.05$, **$p<0.01$, ***$p<0.001$), two-tailed Student's t-test was used, only if the data sets passed the equal variance test (Levene Median test) and normality test (Kolmogorov-Smirnov test) (SigmaStat 3.0.). When the data set did not meet the assumptions of a parametric test, Mann-Whitney Rank Sum Test was performed. The correlation between gliosis and X-34 plaque load was analyzed with Pearson product moment correlation test (SigmaStat 3.0.). Variability of the measurements was reported as SEM.

## Supplementary Material

Refer to Web version on PubMed Central for supplementary material.

## Acknowledgments

This work was supported by the American Health Assistance Foundation (JK and DMH), NIH grants AG13956 (DMH), AG034004-01A1 (JMC), NIH Neuroscience Blueprint Center Core Grant P30 NS057105, the Alafi Neuroimaging Laboratory, and Eli Lilly.

## References

Andersen K, Launer LJ, Dewey ME, Letenneur L, Ott A, Copeland JR, Dartigues JF, Kragh-Sorensen P, Baldereschi M, Brayne C, et al. Gender differences in the incidence of AD and vascular dementia: The EURODEM Studies. EURODEM Incidence Research Group. Neurology 1999;53:1992–1997. [PubMed: 10599770]

Bales KR, Verina T, Cummins DJ, Du Y, Dodel RC, Saura J, Fishman CE, DeLong CA, Piccardo P, Petegnief V, et al. Apolipoprotein E is essential for amyloid deposition in the APP(V717F) transgenic mouse model of Alzheimer's disease. Proc Natl Acad Sci USA 1999;96:15233–15238. [PubMed: 10611368]

Bales KR, Verina T, Dodel RC, Du Y, Altstiel L, Bender M, Hyslop P, Johnstone EM, Little SP, Cummins DJ, et al. Lack of apolipoprotein E dramatically reduces amyloid beta-peptide deposition. Nat Genet 1997;17:263–264. [PubMed: 9354781]

Bell RD, Sagare AP, Friedman AE, Bedi GS, Holtzman DM, Deane R, Zlokovic BV. Transport pathways for clearance of human Alzheimer's amyloid beta-peptide and apolipoproteins E and J in the mouse central nervous system. J Cereb Blood Flow Metab 2007;27:909–918. [PubMed: 17077814]

Bertram L, Hsiao M, McQueen MB, Parkinson M, Mullin K, Blacker D, Tanzi RE. The LDLR locus in Alzheimer's disease: a family-based study and meta-analysis of case-control data. Neurobiol Aging 2007a;28(18):e11–14.

Bertram L, McQueen MB, Mullin K, Blacker D, Tanzi RE. Systematic meta-analyses of Alzheimer disease genetic association studies: the AlzGene database. Nat Genet 2007b;39:17–23. [PubMed: 17192785]

Borchelt DR, Davis J, Fischer M, Lee MK, Slunt HH, Ratovitsky T, Regard J, Copeland NG, Jenkins NA, Sisodia SS, Price DL. A vector for expressing foreign genes in the brains and hearts of transgenic mice. Genet Anal 1996;13:159–163. [PubMed: 9117892]

Brown MS, Goldstein JL. A receptor-mediated pathway for cholesterol homeostasis. Science 1986;232:34–47. [PubMed: 3513311]

Callahan MJ, Lipinski WJ, Bian F, Durham RA, Pack A, Walker LC. Augmented senile plaque load in aged female beta-amyloid precursor protein-transgenic mice. Am J Pathol 2001;158:1173–1177. [PubMed: 11238065]

Cam JA, Bu G. Modulation of beta-amyloid precursor protein trafficking and processing by the low density lipoprotein receptor family. Mol Neurodegener 2006;1:8. [PubMed: 16930455]

Cao D, Fukuchi K, Wan H, Kim H, Li L. Lack of LDL receptor aggravates learning deficits and amyloid deposits in Alzheimer transgenic mice. Neurobiol Aging 2006;27:1632–1643. [PubMed: 16236385]

Carroll JC, Rosario ER, Chang L, Stanczyk FZ, Oddo S, LaFerla FM, Pike CJ. Progesterone and estrogen regulate Alzheimer-like neuropathology in female 3xTg-AD mice. J Neurosci 2007;27:13357–13365. [PubMed: 18045930]

Cheng D, Huang R, Lanham IS, Cathcart HM, Howard M, Corder EH, Poduslo SE. Functional interaction between APOE4 and LDL receptor isoforms in Alzheimer's disease. J Med Genet 2005;42:129–131. [PubMed: 15689450]

Cirrito JR, May PC, O'Dell MA, Taylor JW, Parsadanian M, Cramer JW, Audia JE, Nissen JS, Bales KR, Paul SM, et al. In vivo assessment of brain interstitial fluid with microdialysis reveals plaque-

associated changes in amyloid-beta metabolism and half-life. J Neurosci 2003;23:8844–8853. [PubMed: 14523085]

Cole SL, Vassar R. The Alzheimer's disease Beta-secretase enzyme, BACE1. Mol Neurodegener 2007;2:22. [PubMed: 18005427]

Deane R, Sagare A, Hamm K, Parisi M, Lane S, Finn MB, Holtzman DM, Zlokovic BV. apoE isoform-specific disruption of amyloid beta peptide clearance from mouse brain. J Clin Invest 2008;118:4002–4013. [PubMed: 19033669]

DeMattos RB, Cirrito JR, Parsadanian M, May PC, O'Dell MA, Taylor JW, Harmony JA, Aronow BJ, Bales KR, Paul SM, Holtzman DM. ApoE and clusterin cooperatively suppress Abeta levels and deposition: evidence that ApoE regulates extracellular Abeta metabolism in vivo. Neuron 2004;41:193–202. [PubMed: 14741101]

DeMattos RB, O'Dell MA, Parsadanian M, Taylor JW, Harmony JA, Bales KR, Paul SM, Aronow BJ, Holtzman DM. Clusterin promotes amyloid plaque formation and is critical for neuritic toxicity in a mouse model of Alzheimer's disease. Proc Natl Acad Sci USA 2002;99:10843–10848. [PubMed: 12145324]

Elder GA, Cho JY, English DF, Franciosi S, Schmeidler J, Sosa MA, Gasperi RD, Fisher EA, Mathews PM, Haroutunian V, Buxbaum JD. Elevated plasma cholesterol does not affect brain Abeta in mice lacking the low-density lipoprotein receptor. J Neurochem 2007;102:1220–1231. [PubMed: 17472705]

Filipovic I. Effect of inhibiting N-glycosylation on the stability and binding activity of the low density lipoprotein receptor. J Biol Chem 1989;264:8815–8820. [PubMed: 2722801]

Fryer JD, Demattos RB, McCormick LM, O'Dell MA, Spinner ML, Bales KR, Paul SM, Sullivan PM, Parsadanian M, Bu G, Holtzman DM. The low density lipoprotein receptor regulates the level of central nervous system human and murine apolipoprotein E but does not modify amyloid plaque pathology in PDAPP mice. J Biol Chem 2005;280:25754–25759. [PubMed: 15888448]

Golde TE. Disease modifying therapy for AD? J Neurochem 2006;99:689–707. [PubMed: 17076654]

Gopalraj RK, Zhu H, Kelly JF, Mendiondo M, Pulliam JF, Bennett DA, Estus S. Genetic association of low density lipoprotein receptor and Alzheimer's disease. Neurobiol Aging 2005;26:1–7. [PubMed: 15585340]

Halford RW, Russell DW. Reduction of cholesterol synthesis in the mouse brain does not affect amyloid formation in Alzheimer's disease, but does extend lifespan. Proc Natl Acad Sci USA 2009;106:3502–3506. [PubMed: 19204288]

Hardy J. A hundred years of Alzheimer's disease research. Neuron 2006;52:3–13. [PubMed: 17015223]

Herz J. Apolipoprotein E receptors in the nervous system. Curr Opin Lipidol 2009;20:190–196. [PubMed: 19433918]

Herz J, Bock HH. Lipoprotein receptors in the nervous system. Annu Rev Biochem 2002;71:405–434. [PubMed: 12045102]

Hirsch-Reinshagen V, Maia LF, Burgess BL, Blain JF, Naus KE, McIsaac SA, Parkinson PF, Chan JY, Tansley GH, Hayden MR, et al. The absence of ABCA1 decreases soluble ApoE levels but does not diminish amyloid deposition in two murine models of Alzheimer disease. J Biol Chem 2005;280:43243–43256. [PubMed: 16207707]

Hofmann SL, Russell DW, Brown MS, Goldstein JL, Hammer RE. Overexpression of low density lipoprotein (LDL) receptor eliminates LDL from plasma in transgenic mice. Science 1988;239:1277–1281. [PubMed: 3344433]

Holtzman DM, Bales KR, Tenkova T, Fagan AM, Parsadanian M, Sartorius LJ, Mackey B, Olney J, McKeel D, Wozniak D, Paul SM. Apolipoprotein E isoform-dependent amyloid deposition and neuritic degeneration in a mouse model of Alzheimer's disease. Proc Natl Acad Sci USA 2000a; 97:2892–2897. [PubMed: 10694577]

Holtzman DM, Fagan AM, Mackey B, Tenkova T, Sartorius L, Paul SM, Bales K, Ashe KH, Irizarry MC, Hyman BT. Apolipoprotein E facilitates neuritic and cerebrovascular plaque formation in an Alzheimer's disease model. Ann Neurol 2000b;47:739–747. [PubMed: 10852539]

Jankowsky JL, Fadale DJ, Anderson J, Xu GM, Gonzales V, Jenkins NA, Copeland NG, Lee MK, Younkin LH, Wagner SL, et al. Mutant presenilins specifically elevate the levels of the 42 residue

beta-amyloid peptide in vivo: evidence for augmentation of a 42-specific gamma secretase. Hum Mol Genet 2004;13:159–170. [PubMed: 14645205]

Jiang Q, Lee CY, Mandrekar S, Wilkinson B, Cramer P, Zelcer N, Mann K, Lamb B, Willson TM, Collins JL, et al. ApoE promotes the proteolytic degradation of Abeta. Neuron 2008;58:681–693. [PubMed: 18549781]

Kim J, Basak JM, Holtzman DM. The role of apolipoprotein E in Alzheimer's disease. Neuron 2009;63:287–303. [PubMed: 19679070]

Kim J, Onstead L, Randle S, Price R, Smithson L, Zwizinski C, Dickson DW, Golde T, McGowan E. Abeta40 Inhibits Amyloid Deposition In Vivo. J Neurosci 2007;27:627–633. [PubMed: 17234594]

Koldamova R, Staufenbiel M, Lefterov I. Lack of ABCA1 considerably decreases brain ApoE level and increases amyloid deposition in APP23 mice. J Biol Chem 2005;280:43224–43235. [PubMed: 16207713]

Krul ES, Tikkanen MJ, Schonfeld G. Heterogeneity of apolipoprotein E epitope expression on human lipoproteins: importance for apolipoprotein E function. J Lipid Res 1988;29:1309–1325. [PubMed: 2466929]

Lämsä R, Helisalmi S, Herukka SK, Tapiola T, Pirttilä T, Vepsäläinen S, Hiltunen M, Soininen H. Genetic study evaluating LDLR polymorphisms and Alzheimer's disease. Neurobiol Aging 2008;29:848–855. [PubMed: 17239995]

Liu Q, Zerbinatti CV, Zhang J, Hoe HS, Wang B, Cole SL, Herz J, Muglia L, Bu G. Amyloid Precursor Protein Regulates Brain Apolipoprotein E and Cholesterol Metabolism through Lipoprotein Receptor LRP1. Neuron 2007;56:66–78. [PubMed: 17920016]

Mahley RW, Ji ZS. Remnant lipoprotein metabolism: key pathways involving cell-surface heparan sulfate proteoglycans and apolipoprotein E. J Lipid Res 1999;40:1–16. [PubMed: 9869645]

Menacherry S, Hubert W, Justice JB Jr. In vivo calibration of microdialysis probes for exogenous compounds. Anal Chem 1992;64:577–583. [PubMed: 1580357]

Meyer-Luehmann M, Spires-Jones TL, Prada C, Garcia-Alloza M, de Calignon A, Rozkalne A, Koenigsknecht-Talboo J, Holtzman DM, Bacskai BJ, Hyman BT. Rapid appearance and local toxicity of amyloid-beta plaques in a mouse model of Alzheimer's disease. Nature 2008;451:720–724. [PubMed: 18256671]

Meyer-Luehmann M, Stalder M, Herzig MC, Kaeser SA, Kohler E, Pfeifer M, Boncristiano S, Mathews PM, Mercken M, Abramowski D, et al. Extracellular amyloid formation and associated pathology in neural grafts. Nat Neurosci 2003;6:370–377. [PubMed: 12598899]

Pietrzik CU, Busse T, Merriam DE, Weggen S, Koo EH. The cytoplasmic domain of the LDL receptor-related protein regulates multiple steps in APP processing. Embo J 2002;21:5691–5700. [PubMed: 12411487]

Quan G, Xie C, Dietschy JM, Turley SD. Ontogenesis and regulation of cholesterol metabolism in the central nervous system of the mouse. Brain Res Dev Brain Res 2003;146:87–98.

Retz W, Thome J, Durany N, Harsanyi A, Retz-Junginger P, Kornhuber J, Riederer P, Rosler M. Potential genetic markers of sporadic Alzheimer's dementia. Psychiatr Genet 2001;11:115–122. [PubMed: 11702052]

Rodriguez E, Mateo I, Llorca J, Sanchez-Quintana C, Infante J, Berciano J, Combarros O. No association between low density lipoprotein receptor genetic variants and Alzheimer's disease risk. Am J Med Genet B Neuropsychiatr Genet 2006;141B:541–543. [PubMed: 16741934]

Sisodia SS, St George-Hyslop PH. gamma-Secretase, Notch, Abeta and Alzheimer's disease: where do the presenilins fit in? Nat Rev Neurosci 2002;3:281–290. [PubMed: 11967558]

Soutar AK, Naoumova RP. Mechanisms of disease: genetic causes of familial hypercholesterolemia. Nat Clin Pract Cardiovasc Med 2007;4:214–225. [PubMed: 17380167]

Steiner H, Haass C. Intramembrane proteolysis by presenilins. Nat Rev Mol Cell Biol 2000;1:217–224. [PubMed: 11252897]

Taha AY, Chen CT, Liu Z, Kim JH, Mount HT, Bazinet RP. Brainstem Concentrations of Cholesterol are not Influenced by Genetic Ablation of the Low-Density Lipoprotein Receptor. Neurochem Res 2008;34:311–315. [PubMed: 18607722]

Tamboli IY, Prager K, Thal DR, Thelen KM, Dewachter I, Pietrzik CU, St George-Hyslop P, Sisodia SS, De Strooper B, Heneka MT, et al. Loss of gamma-Secretase Function Impairs Endocytosis of

Lipoprotein Particles and Membrane Cholesterol Homeostasis. J Neurosci 2008;28:12097–12106. [PubMed: 19005074]

Ulery PG, Beers J, Mikhailenko I, Tanzi RE, Rebeck GW, Hyman BT, Strickland DK. Modulation of beta-amyloid precursor protein processing by the low density lipoprotein receptor-related protein (LRP). Evidence that LRP contributes to the pathogenesis of Alzheimer's disease. J Biol Chem 2000;275:7410–7415. [PubMed: 10702315]

Wahrle SE, Jiang H, Parsadanian M, Hartman RE, Bales KR, Paul SM, Holtzman DM. Deletion of Abca1 increases Abeta deposition in the PDAPP transgenic mouse model of Alzheimer disease. J Biol Chem 2005;280:43236–43242. [PubMed: 16207708]

Wahrle SE, Jiang H, Parsadanian M, Kim J, Li A, Knoten A, Jain S, Hirsch-Reinshagen V, Wellington CL, Bales KR, et al. Overexpression of ABCA1 reduces amyloid deposition in the PDAPP mouse model of Alzheimer disease. J Clin Invest 2008;118:671–682. [PubMed: 18202749]

Wang J, Tanila H, Puolivali J, Kadish I, van Groen T. Gender differences in the amount and deposition of amyloidbeta in APPswe and PS1 double transgenic mice. Neurobiol Dis 2003;14:318–327. [PubMed: 14678749]

Wouters K, Shiri-Sverdlov R, van Gorp PJ, van Bilsen M, Hofker MH. Understanding hyperlipidemia and atherosclerosis: lessons from genetically modified apoe and ldlr mice. Clin Chem Lab Med 2005;43:470–479. [PubMed: 15899668]

Wyss-Coray T. Inflammation in Alzheimer disease: driving force, bystander or beneficial response? Nat Med 2006;12:1005–1015. [PubMed: 16960575]

Yokode M, Hammer RE, Ishibashi S, Brown MS, Goldstein JL. Diet-induced hypercholesterolemia in mice: prevention by overexpression of LDL receptors. Science 1990;250:1273–1275. [PubMed: 2244210]

Yue X, Lu M, Lancaster T, Cao P, Honda S, Staufenbiel M, Harada N, Zhong Z, Shen Y, Li R. Brain estrogen deficiency accelerates Abeta plaque formation in an Alzheimer's disease animal model. Proc Natl Acad Sci USA 2005;102:19198–19203. [PubMed: 16365303]

Zerbinatti CV, Wahrle SE, Kim H, Cam JA, Bales K, Paul SM, Holtzman DM, Bu G. Apolipoprotein E and low density lipoprotein receptor-related protein facilitate intraneuronal Abeta42 accumulation in amyloid model mice. J Biol Chem 2006;281:36180–36186. [PubMed: 17012232]

Zerbinatti CV, Wozniak DF, Cirrito J, Cam JA, Osaka H, Bales KR, Zhuo M, Paul SM, Holtzman DM, Bu G. Increased soluble amyloid-beta peptide and memory deficits in amyloid model mice overexpressing the low-density lipoprotein receptor-related protein. Proc Natl Acad Sci USA 2004;101:1075–1080. [PubMed: 14732699]

Zou F, Gopalraj RK, Lok J, Zhu H, Ling IF, Simpson JF, Tucker HM, Kelly JF, Younkin SG, Dickson DW, et al. Sex-dependent Association of a Common Low Density Lipoprotein Receptor Polymorphism with RNA Splicing Efficiency in the Brain and Alzheimers Disease. Hum Mol Genet 2008;17:929–935. [PubMed: 18065781]

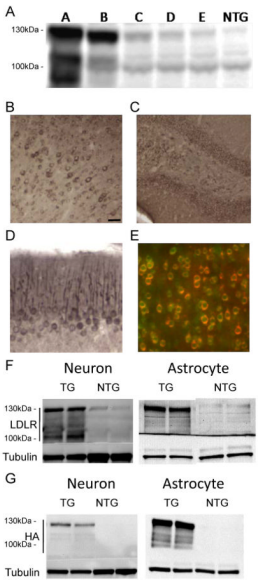


**Figure 1. Expression of LDLR Transgene in Neurons and Astrocytes**

(A) Levels of LDLR protein in the cortex of 5 different LDLR transgenic lines were assessed by western blotting. RIPA-soluble cortex lysates from LDLR transgenic mice and non-transgenic (NTG) mice were probed with anti-LDLR antibody (Novus). (B–D) Regional expression patterns of LDLR in B line mice were characterized by immunostaining with anti-HA antibody to detect HA-tagged LDLR protein. LDLR was expressed in the cortex (B), dentate gyrus of hippocampus (C), and Purkinje cell dendrites of cerebellum (D). (E–G) Cellular expression profile of the LDLR transgene was examined by using anti-HA or anti-LDLR antibody. (E) Cortical sections were stained by double-immunofluorescence labeling for HA (red) and the neuronal marker NeuN (green). (F) Cell lysates from primary neurons or astrocytes isolated from LDLR B line transgenic (TG) and NTG mice were analyzed by probing with either anti-LDLR (Novus) or anti-LDLR (Dr. Bu) antibody, respectively. (G) Expression of HA-tagged LDLR transgene in primary neurons and astrocytes was confirmed by western blotting with anti-HA antibody. Scale bar: 30μm. See also Figure S1.

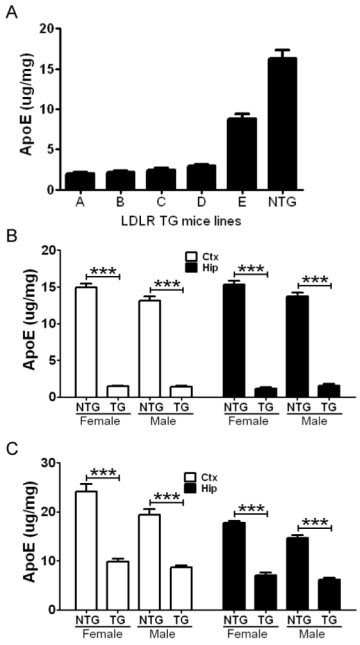


**Figure 2. Reduction of Brain ApoE Protein Levels by LDLR Overexpression**

(A) Cortex from 5 LDLR transgenic lines and NTG mice were homogenized with PBS at 3 months of age. Levels of apoE protein in PBS-extracted fraction were analyzed by apoE ELISA. (n=4 per group) (B) Hemizygous LDLR B line mice were bred with APP/PS1 transgenic mice. Levels of PBS-soluble apoE in the cortex (Ctx) and hippocampus (Hip) were measured from APP/PS1 mice without the LDLR transgene (NTG) and from APP/PS1/LDLR (TG) mice. To prevent any confounding effect from amyloid plaque formation and sex difference, mice were analyzed by sex at 2.5 months of age. (n=5–10 per group) (C) The progeny of hemizygous LDLR E line bred with APP/PS1 mice were similarly analyzed for apoE protein levels in the Ctx and Hip. There was a 55–60% reduction of apoE levels in LDLR TG mice, compared with NTG mice. (n=6–8 per group) Values are mean ± SEM. See also Figure S2 and S3.

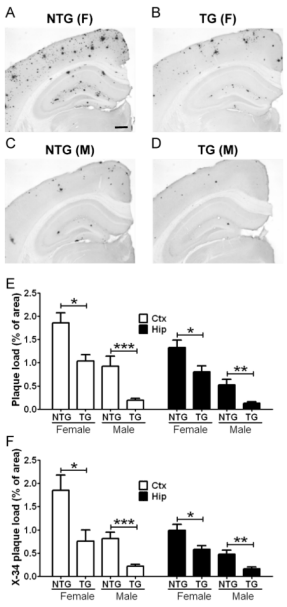


**Figure 3. Inhibition of Plaque Formation by Strong LDLR Overexpression**

Brain sections from APP/PS1 mice without LDLR transgene (NTG) (A and C) and APP/PS1/LDLR B line transgenic mice (TG) (B and D) were immunostained for Aβ using the 3D6 antibody. Scale bar: 300μm. (E) The extent of plaque deposition detected by 3D6 antibody was quantified from cortex (Ctx) and hippocampus (Hip) of APP/PS1 and APP/PS1/LDLR transgenic mice. Female and male mice were analyzed separately at 7 months of age. (n=6–12 per group) (F) Brain sections from APP/PS1 and APP/PS1/LDLR TG mice were stained with X-34 dye that recognizes compact fibrillar plaques. X-34 positive fibrillar plaque loads in the Ctx and Hip were analyzed by applying an unbiased stereological method. (n=6–12 per group)

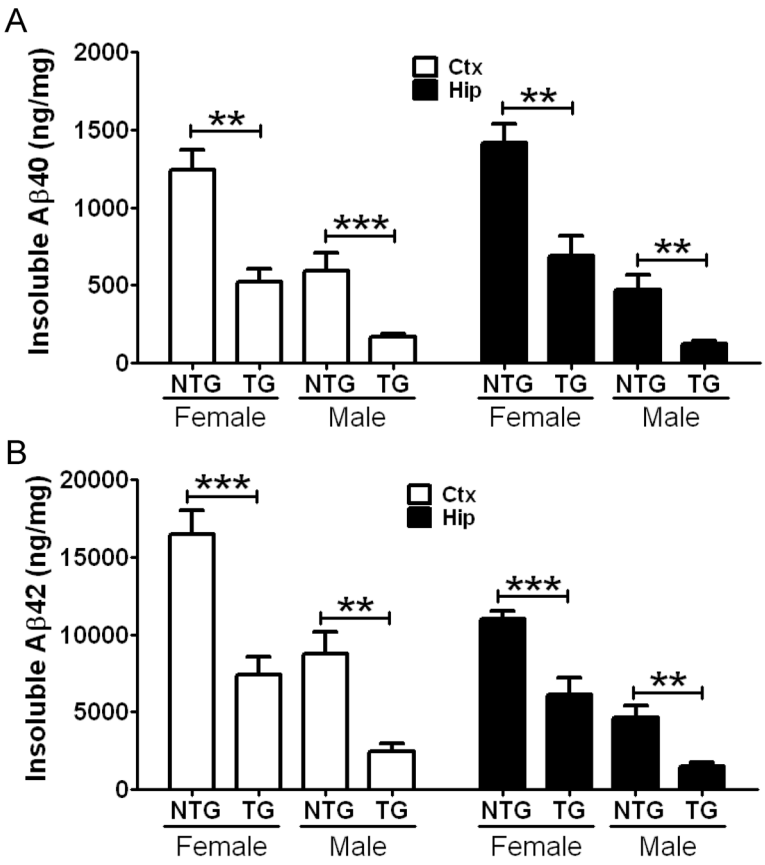


**Figure 4. Decrease of Aβ Accumulation in APP/PS1/LDLR Transgenic Mice**

Cortical (Ctx) and hippocampal (Hip) tissues from 7 month old APP/PS1 (NTG) and APP/PS1/LDLR B line transgenic mice (TG) were sequentially homogenized by using PBS and guanidine buffer. PBS-insoluble Aβ40 (A) and Aβ42 (B) levels were measured from Ctx and Hip by using a sandwich Aβ ELISA. (n=6–12 per group) Values are mean ± SEM. See also Table S1.

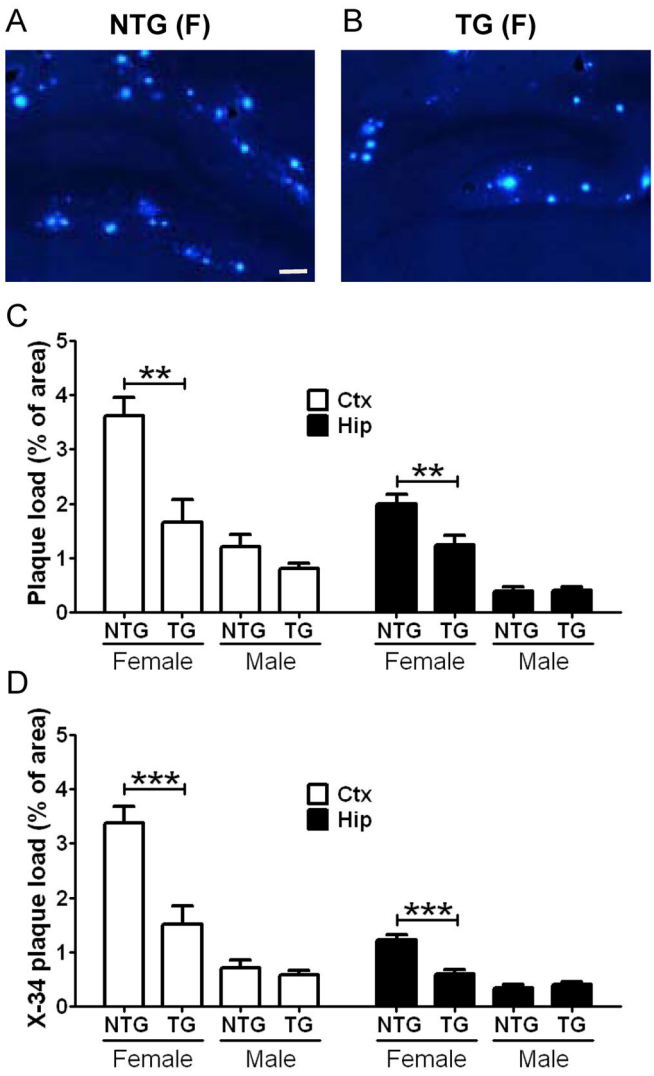


**Figure 5. Two-fold Overexpression of LDLR Prevents Amyloid Formation**

Hippocampal sections from 7 month old female APP/PS1 (NTG) (A) and APP/PS1/LDLR E line transgenic mice (TG) (B) were stained with fibrillar plaque-specific X-34 dye. Scale bar: 100μm. (C) The extent of plaque deposition detected by 3D6 antibody was quantified from cortex (Ctx) and hippocampus (Hip) of APP/PS1 and APP/PS1/LDLR E line transgenic mice. There was no statistically significant difference between genotypes in male mice. (D) X-34 positive fibrillar plaque load was analyzed from Ctx and Hip of APP/PS1 and APP/PS1/LDLR transgenic mice. (n=8–13 per group) See also Table S1.

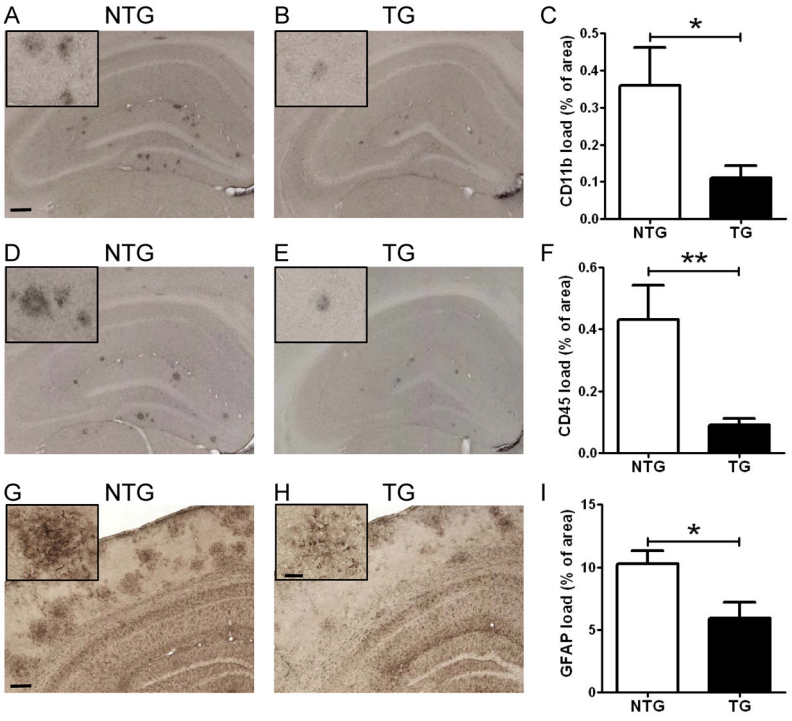


**Figure 6. Attenuation of Neuroinflammatory Responses in APP/PS1/LDLR Mice**

Hippocampal sections from male APP/PS1 (NTG) and APP/PS1/LDLR B line transgenic mice (TG) were immunostained with an antibody against the microglial marker CD11b (A–B) and CD45 (D–E). Scale bar: 150μm. The percent area covered by CD11b staining (C) and CD45 staining (F) was quantified from APP/PS1 and APP/PS1/LDLR B line. (n=8–10 per group) Cortical sections from female APP/PS1 (G) and APP/PS1/LDLR B line transgenic mice (H) were immunostained with anti-GFAP antibody, a marker of astrogliosis. Scale bar: 180μm. (I) The percent area covered by GFAP staining was quantified. (n=6–8 per group) Scale bar for higher magnification inserts: 40μm. All mice were 7 month old. See also Figure S4.

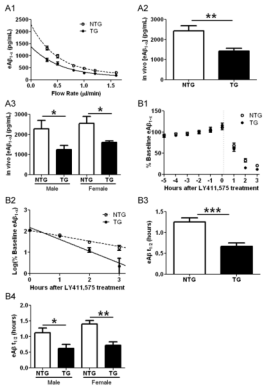

**Figure 7. Steady State ISF eAβ Levels and Elimination Half-life Are Altered in APP/PS1 Mice Overexpressing LDLR**

(A1) An exponential decay regression was used to fit the concentrations of $eA\beta_{1\text{-}x}$ obtained at each flow rate for individual mice in both groups. The equations of the individual regressions were used to calculate the value at X=0 for each mouse in both groups. (A2) The mean in vivo steady state concentrations for ISF $eA\beta_{1\text{-}x}$ (in pg/mL) calculated from the method in A1 were 2426 ± 260.5 and 1432 ± 124.8 for APP/PS1 (NTG) and APP/PS1/LDLR (TG) mice, respectively (n=12 per group; p=0.0036, student's *t* test with Welch's correction). (A3) The mean in vivo steady state concentrations for ISF $eA\beta_{1\text{-}x}$ (in pg/mL) were significantly lower in APP/PS1/LDLR (TG) mice than in APP/PS1 (NTG) mice when comparing within the same sex (n=6 per group; p=0.049 and 0.040 for male and female comparisons, respectively) (B1) After a six-hour baseline of ISF $eA\beta_{1\text{-}x}$ was achieved, levels of the peptide rapidly decreased for both groups studied within several hours of a 10 mg/kg i.p. injection of the gamma secretase inhibitor LY411,575. (B2) The plot of the common logarithm of percent baseline ISF $eA\beta_{1\text{-}x}$ concentrations versus time was linear in both groups studied, suggesting net first-order kinetics. Data shown represent timepoints at which Aβ levels had not yet plateaued. The slope from the individual linear regressions from log(% eAβ) vs. time for each mouse was used to calculate the mean half-life ($t_{1/2}$) of elimination for eAβ from the ISF in (B3). (B3) The mean $eA\beta t_{1/2}$ (in hours) was 1.25 ± 0.0989 (n=13) and 0.671 ± 0.0833 (n = 12) in NTG and TG mice, respectively. (B4) In NTG and TG male mice, the $eA\beta t_{1/2}$ (in hours) was 1.13 ± 0.147 (n=7) and 0.625 ± 0.126 (n=6), respectively. In NTG and TG female mice, the $eA\beta t_{1/2}$ (in hours) was 1.39 ± 0.112 (n=6) and 0.717 ± 0.117 (n=6), respectively. Differences were significant for comparisons between males as well as those made for females of each genotype (p=0.028 and 0.0018, respectively). See also Figure S5 and Table S2.